

# Far-infrared Absorption Spectra and Properties of SnO<sub>2</sub> Nanorods

Liu Y. K.<sup>1</sup> Dong Y.<sup>2</sup> Wang G. H.<sup>2</sup>

(1 National Laboratory of Solid State Microstructures and Department of Physics, Nanjing University, Nanjing 210093; Structural Research Laboratory, University of Science and Technology of China, Hefei, Anhui 230026; and Department of Physics, Yunnan Normal University, Kunming 650092; 2 National Laboratory of Solid State Microstructures and Department of Physics, Nanjing University, Nanjing 210093)

Nanostructured materials have drawn considerable attention because they are promising candidates for next-generation electronic and photonic devices with low power consumption<sup>[1-5]</sup>. A number of methods, such as laser ablation<sup>[6]</sup>, template-induced growth<sup>[7]</sup>, arc discharge<sup>[8]</sup>, vapor transport<sup>[9]</sup>, and molecular-beam epitaxy<sup>[10]</sup>, have been developed to synthesize Si, Ge, MgO, SnO<sub>2</sub>, GaN, and Ga<sub>2</sub>O<sub>3</sub> nanowires or nanorods<sup>[11-13]</sup>. From the viewpoint of dimensionality, one-dimensional (1D) nanostructures are expected to exhibit electronic and optical properties that strongly depend on size and geometry. In addition, the surface effect becomes important in thinner nanorods. Of these 1D nanomaterials, stannic oxide is the most important base material for applications such as gas sensors, transistors, electrode materials<sup>[14,17]</sup>, and more recently, solar cells<sup>[18]</sup>, because of optical conductivity of its film. However, until now, far-infrared (FIR) properties of SnO<sub>2</sub> nanorods have been little explored. In this paper, we report conspicuous FIR absorption spectrum platform peaks of SnO<sub>2</sub> nanorods with widths of up to 61.6 and 119 cm<sup>-1</sup> due to the overlap of the surface vibration modes, both from the cylindrical nanorods and a smaller amount of spheroid particles.

The two samples were synthesized by redox reaction<sup>[19]</sup> under different annealing conditions. Sample A, 20 nm in diameter, was synthesized by annealing precursors (which were produced in a microemulsion) at a heating rate of 5°C/min, up to 780°C for 30 min. Sample B, 45 nm in diameter, was prepared at a heating rate of 20°C/min, up to 780°C for 60 min. The structural properties of the SnO<sub>2</sub> nanorods were examined by x-ray diffraction (XRD), transmission electron microscopy (TEM), and high-resolution transmission electron microscopy (HRTEM). The FIR absorption spectrum was investigated by IFS 66V and Nexus 870 FT-IR.

Fig. 1 shows the XRD patterns of samples A and B.

The sharp diffraction peaks in the patterns can be indexed to a rutile structure, in agreement with the reported data of bulk SnO<sub>2</sub> ( $a=b=4.738\text{Å}$ ,  $c=3.188\text{Å}$ , and JCPD 21-1252), but the diffraction peaks of sample A are broadened due to its small diameter.

Fig. 2 shows TEM images revealing the general morphology of the SnO<sub>2</sub> nanorods. Most nanorods of sample A Fig. 2 (a) have diameters around 20 nm and lengths about several micrometers. The HRTEM image is shown in Fig. 2 (c); the lattice planes of (101) and (200) with interplanar spacings of 2.55 and 2.37Å respectively, are clearly displayed. For sample B, the diameter is 45 nm, and the length is 5-10 μm, as shown in Fig. 2(b).

Fig. 3 and 4 show FIR absorption of samples spectra A and B. Two obvious features can be easily found. (1) Two FIR platform peaks at 249.5-268.9 and 289.3-350.9 cm<sup>-1</sup> of sample A in the range of 75 to 400 cm<sup>-1</sup> are observed, and the width of the latter peak is up to 61.6 cm<sup>-1</sup>. The FIR spectrum for sample B is similar to that for sample A, but the widths of the FIR platform

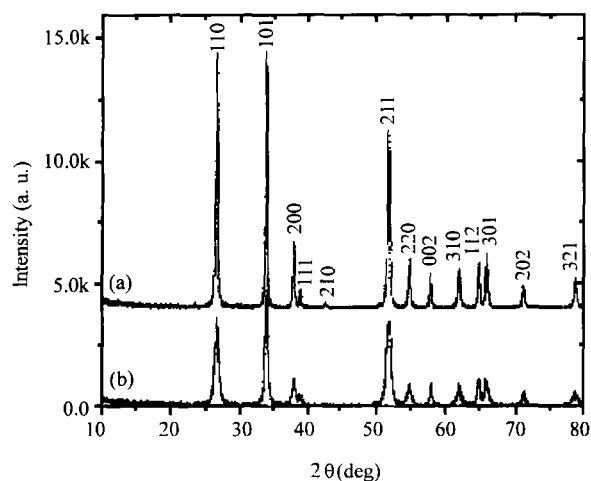
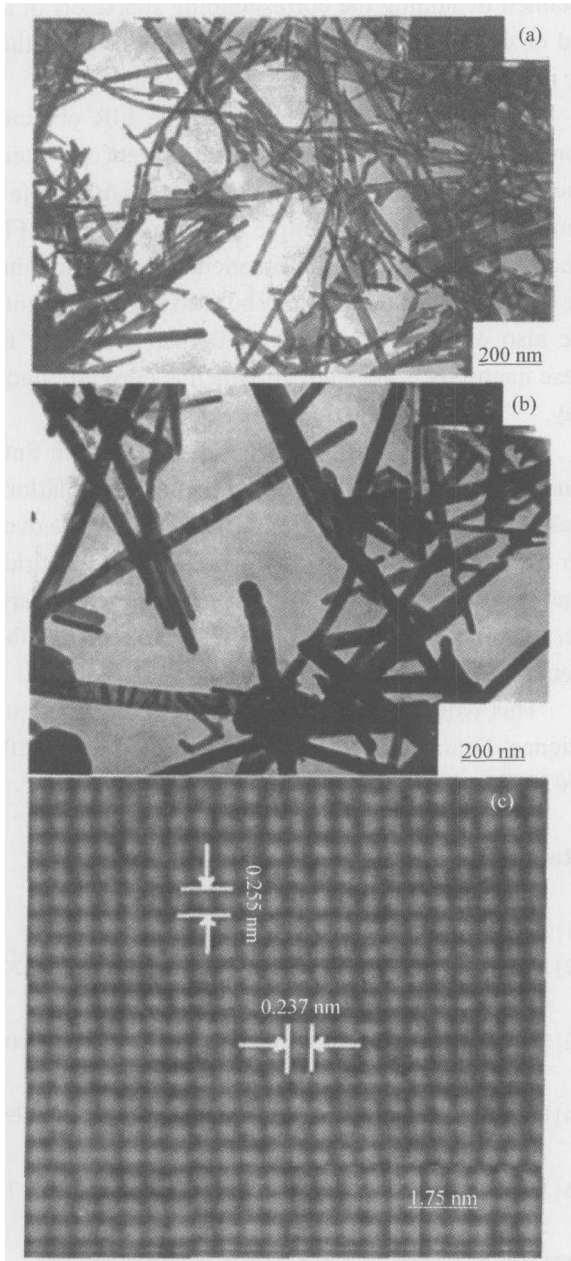


Fig. 1 XRD patterns of SnO<sub>2</sub> nanorods. (a) Sample A. (b) Sample B.

SCIENCE FOUNDATION IN CHINA



**Fig. 2 TEM and HRTEM images of SnO<sub>2</sub> nanorods. (a) Sample A. (b) Sample B. (c) HRTEM of a single nanorod in sample A.**

peaks at 252.1-271.7 and 295.2-351.7 cm<sup>-1</sup> are narrower than those of sample A, indicating that there are more surface modes in sample A. (2) In the range of 400 to 1200 cm<sup>-1</sup>, the FIR spectrum of sample A exhibits two platform peaks at 479.2-598.2 and 613.6-678.3 cm<sup>-1</sup>, respectively, and the width of the first peak is up to 119 cm<sup>-1</sup>, whereas for sample B two asymmetric peaks exist at 474.8 and 680.3 cm<sup>-1</sup> without FIR platform peaks, which is in good agreement with those for SnO<sub>2</sub> bulk and particle<sup>[20,21]</sup>.

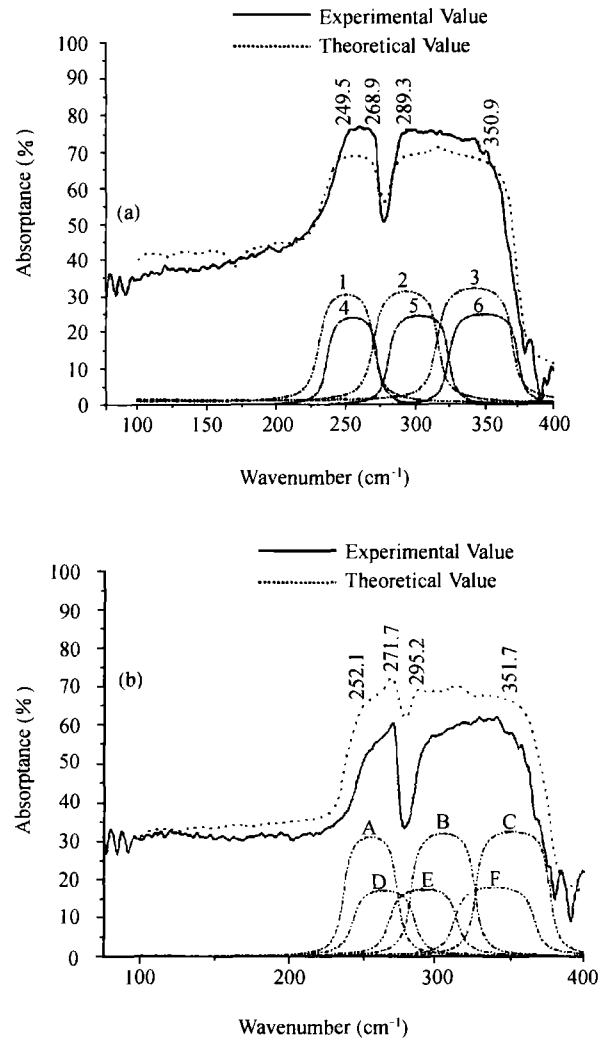


**Fig. 3 FIR absorption spectra of SnO<sub>2</sub> nanorods. (a) Sample A in the range of 75 to 400 cm<sup>-1</sup>. (b) Sample B in the range of 75 to 400 cm<sup>-1</sup>.**

Now let us look at the origin of these FIR platform peaks of samples A and B. The appearance of the low-frequency FIR platform peaks brings to mind the results reported by Fuchs et al.<sup>[22]</sup>, Yamamoto et al.<sup>[23]</sup>, Ruppin et al.<sup>[24,25]</sup> and Luxon et al.<sup>[26]</sup>, who have observed low-frequency FIR platform peaks resulting from the surface modes of cylindrical and spheroid particles. These pioneers have theoretically and experimentally studied these FIR platform peaks. For spheroid particles, the value of the surface modes  $\bar{\omega}$ , given by<sup>[23]</sup>

$$\bar{\omega}_s^2 = \frac{\epsilon_0 + (n+1)\epsilon_m}{\epsilon_\infty + (n+1)\epsilon_m} \omega_{TO}^2 \quad (1)$$

For cylindrical particles, the value of the surface modes<sup>[23]</sup>  $\omega_c$  given by

$$\omega_c^2 = \frac{\epsilon_0 + \epsilon_m}{\epsilon_\infty + \epsilon_m} \omega_{TO}^2 \quad (2)$$

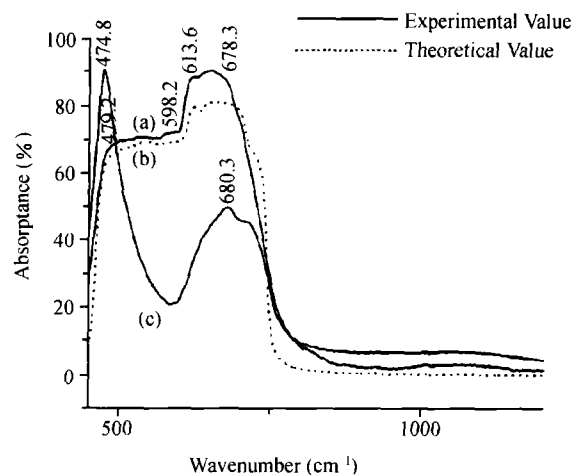


**Fig.4** FIR absorption spectra of SnO<sub>2</sub> nanorods in the range of 400 to 1200 cm<sup>-1</sup>. (a), (b) Sample A; (c) Sample B.

The coupling modes  $\bar{\omega}_s$  and  $\bar{\omega}_c$ , extending over a finite range of wave numbers, contribute a Lorentzian peak to the extinction cross section<sup>[23]</sup>. The overlapped peaks corresponding to  $\bar{\omega}_s$  and  $\bar{\omega}_c$  lead to the emergence of FIR platform peaks. The quantity ratio of spheroid to cylindrical nanorods in our samples is about 0.2. Therefore, we can use formulas (1) and (2) to calculate  $\bar{\omega}_s$  and  $\bar{\omega}_c$  for  $\bar{\omega}_{TO}$  of both samples A and B. In the range of 75 to 400 cm<sup>-1</sup>, the theoretical values of cylindrical  $\bar{\omega}_{TO}$  of sample A are 72, 84, 99, 116.5, 138.5, 162, 187, 219, and 256 cm<sup>-1</sup>; the theoretical values of spheroid  $\bar{\omega}_{TO}$  are 208, 247, and 285 cm<sup>-1</sup>. The curves marked with 1, 2, and 3 correspond to the cylindrical subpanels of  $\bar{\omega}_s$  when  $\bar{\omega}_{TO}$ =187, 219, and 256 cm<sup>-1</sup>, respectively. Those marked with 4, 5, and 6 correspond to the spheroid subpanels of  $\bar{\omega}_c$  when  $\bar{\omega}_{TO}$ =208, 247, and 285 cm<sup>-1</sup>, respectively, as shown in Fig. 3 (a). Whereas the theoretical values of cylindrical  $\bar{\omega}_{TO}$  of sample B are 74, 86.5, 102, 120, 141, 165, 197, 217, and 253 cm<sup>-1</sup>, the theoretical values of spheroid  $\bar{\omega}_{TO}$  are 208, 248, and 286.5 cm<sup>-1</sup>. The curves marked with A, B, and C of Fig.3(b) correspond to the cylindrical sub-panels of  $\bar{\omega}_c$  when  $\bar{\omega}_{TO}$ =197, 217, and 253 cm<sup>-1</sup>; those marked with D, E, and F correspond to the spheroid subpanels of  $\bar{\omega}_s$  when  $\bar{\omega}_{TO}$ =208, 248, and 286.5 cm<sup>-1</sup>, respectively. In the range of 400 to 1200 cm<sup>-1</sup>, the results of  $\bar{\omega}_{TO}$  for  $\bar{\omega}_c$  of sample A are 375, 439, and 515 cm<sup>-1</sup>; the result of  $\bar{\omega}_{TO}$  for  $\bar{\omega}_s$  is 538 cm<sup>-1</sup>. For sample B, on the other hand, the experimental results are similar to the combinations of those for SnO<sub>2</sub> nanoparticle and bulk, and thus it is not necessary to calculate them. The theoretical results have been

obtained by adding the corresponding subpanels of  $\bar{\omega}_s$  and  $\bar{\omega}_c$  as platform curves illustrated in Fig.3 and 4; they are in good agreement with the experimental values.

A striking difference between the FIR obtained from samples A and B is due to their different diameters. The overlap of the surface vibration modes of sample B is much less than that of sample A. Therefore, the FIR spectra of the sample A are broadened more, and thus the thinner SnO<sub>2</sub> nanorods may be used as FIR detectors. We also observe size effect of Raman scattering for these nanorods, the study of which is currently under way.

In summary, FIR absorption spectra from SnO<sub>2</sub> nanorods have been recorded. The widest FIR platform peak is up to 119 cm<sup>-1</sup> and can be attributed to the overlap of surface vibration modes both from cylindrical nanorods and from a smaller amount of spheroid particles. Excellent agreement between experiments and theoretical calculations has been achieved.

This work was supported by the National Nature Science Foundation of China (Nos. 29890210, 10074024, and 10023001).

## References

- [1] Alivisatos A. P. *Science*, 1996, 271: 993.
- [2] Hu J., T. Odom W., Lieber C. M. *Acc. Chem. Res.*, 1999, 32: 435.
- [3] Sunamura H., Usami N., Shiraki Y. et al. *Appl. Phys. Lett.*, 1996, 68: 13.
- [4] Rakawa T., Kato Y., Sogawa F. et al. *Appl. Phys. Lett.*, 1997, 70: 646.
- [5] Jin G., Tang Y. S., Liu J. et al. *Appl. Phys. Lett.*, 1999, 74: 2471.
- [6] Duan X., Lieber C. J. *Am. Chem. Soc.*, 2000, 122: 188.
- [7] Cheng G., Zhang L., Zhu Y. et al. *Appl. Phys. Lett.*, 1999, 75: 2455.
- [8] Iijima S. *London: Nature*, 1991, 354, 54.
- [9] Pan Z. W., Dai Z. R., Wang Z. L. *Science*, 2001, 291: 1947.
- [10] Lee H. G., Jeon H. C., Kang T. W. et al. *Appl. Phys. Lett.*, 2001, 78: 3319.
- [11] Dai Z. R., Pan Z. W., Wang Z. L. *Solid State Commun.*, 2001, 118: 351.
- [12] Han W. Q., Fang S. S., Li Q. Q. et al. *Science*, 1997, 277: 1287.
- [13] Meng G. W., Zhang L. D., Qin Y. et al. *J. Mater. Sci. Lett.*, 1999, 18: 1255.

(continued on page 49)

SCIENCE FOUNDATION IN CHINA

- [13] Metzger R.M. et al. *J. Am. Chem. Soc.*, 1997, 119: 10455.
- [14] Zhou C., Deshpande M.R., Reed M.A. et al. *Appl. Phys. Lett.*, 1997, 71: 611.
- [15] Ellenbogen J.C., Love J.C. P. *IEEE*, 2000, 88: 386.
- [16] Chen J., Reed M.A., Rawlett A.M. et al. *Science*, 1999, 286: 1550.
- [17] Reed M.A., Tour J.M. *Sci. Amer.*, 2000, 282: 68.
- [18] Vilan A., Shanzer A., Cahen D. *Nature*, 2000, 404: 166.
- [19] Vilan A., Ghabboun J., Cahen D. *J. Phys. Chem.*, 2003, B107: 6360.
- [20] Laws G.M., Thornton T.J., Yang J.M. et al. *Phys. Status Solidi*, 2002, B233: 83; *Physica*, 2003, E17: 659.
- [21] Chen H., Lu J.Q., Wu J. et al. *Phys. Rev.*, 2003, B67: 113 408.
- [22] Brandbyge M., Mozos J. L., Ordejon P. et al. *Phys. Rev.*, 2002, B65: 165 401.
- [23] Sanchez-Portal D., Ordejon P., Artacho E. et al. *Int. J. Quantum Chem.*, 1999, 65: 453; *Ordejon P. Phys. Status Solidi*, 2000, B217: 335.
- [24] Taylor J., Guo H., Wang J. *Phys. Rev.*, 2001, B63: 245 407.
- [25] Troullier N., Martins J.L. *Phys. Rev.*, 1991, B43: 1993.
- [26] Sankey O.F., Niklewski D.J. *Phys. Rev.*, 1989, B40: 3979; Artacho E., Sanchez-Portal D., Ordejon P., Garcia A. et al. *Phys. Status Solidi*, 1999, B215: 809.
- [27] Kaun C.C., Larade B., Guo H. *Phys. Rev.*, 2003, B67: 121 411.
- [28] Wold D.J., Haag R., Rampi M.A. et al. *J. Phys. Chem.*, 2002, B106: 2813.
- [29] Stokbro K., J Taylor., Brandbyge M. et al. *Comp. Mater. Sci.*, 2003, 27: 151.
- [30] Chen J., Su J., Wang W. et al. *Physica*, 2003, E16: 17.
- [31] Hohenberg P., Kohn W. *Phys. Rev.*, 1964, 136: 864; Kohn W., Sham L.J. *Phys. Rev.*, 1965, 140: 1133.
- [32] Ceperley D.M., Alder B.J. *Phys. Rev. Lett.*, 1980, 45: 566.
- [33] Perdew J.P., Zunger A. *Phys. Rev.*, 1981, B23: 5048.
- [34] Datta S. *Electronic Transport in Mesoscopic Systems*, (Cambridge University Press, New York, 1995).
- [35] Monkhorst H.J., Pack J.D. *Phys. Rev.*, 1976, B13: 5188.

-----

(continued from page 44)

- [14] Huang M.H., Wu Y., Feick H. et al. *Adv. Mater.*, 2001, 13: 113.
- [15] Choi Y. C., Kim W. S., Park Y. S. et al. *Adv. Mater.*, 2000, 12, 746.
- [16] Li G.J., Zhang X.H., Kawi S. *Sens. Actuators*, 1999, B60: 64.
- [17] Sberveglieri G. *Sens. Actuators*, 1992, B6: 64.
- [18] Lampert C. M. *Sol. Energy Mater. Sol. Cells*, 1991, 6: 1.
- [19] Liu Y. K., Zheng C. L., Wang W. Z. et al. *J. Cryst. Growth*, 2001, 233: 8.
- [20] Katiyar R. S., Dawson P., Hargreave M. M. et al. *J. Phys.*, 1971, C4: 2421; Gervais E., Kress W. *Phys. Rev.*, 1985, B31: 4809; Satto T., Asari T. *J. Phys. Soc. Jpn.*, 1995, 64: 1193.
- [21] Ocan M., Matijevic, *J. Mater. Res.*, 1990, 5: 1083.
- [22] Fuchs R., Kliewer K. L. *J. Opt. Soc. Am.*, 1958, 58: 319.
- [23] Yamamoto K., Tran C.D., Shimizu H. et al. *J. Phys. Soc. Jpn.*, 1977, 42: 587.
- [24] Ruppin R., Nahum J. J. *Phys. Chem. Solids*, 1974, 35: 1311.
- [25] Ruppin R. J. *Phys. Chem. Solids*, 1969, 30: 2357.
- [26] Luxon J. T., Montgomery D. J., Summitt R. *Phys. Rev.*, 1969, 133: 1345.